Natural Hazards **30:** 399–419, 2003.

Use of Geomorphological Information in Indirect Landslide Susceptibility Assessment

C. J. VAN WESTEN, N. RENGERS and R. SOETERS
International Institute for Aerospace Survey and Earth Sciences, ITC, PO Box 6, 7500 AA Enschede, The Netherlands

(Received: 25 April 2001; accepted 17 October 2001)

Abstract. The objective of this paper is to evaluate the importance of geomorphological expert knowledge in the generation of landslide susceptibility maps, using GIS supported indirect bivariate statistical analysis. For a test area in the Alpago region in Italy a dataset was generated at scale 1:5,000. Detailed geomorphological maps were generated, with legends at different levels of complexity. Other factor maps, that were considered relevant for the assessment of landslide susceptibility, were also collected, such as lithology, structural geology, surficial materials, slope classes, land use, distance from streams, roads and houses. The weights of evidence method was used to generate statistically derived weights for all classes of the factor maps. On the basis of these weights, the most relevant maps were selected for the combination into landslide susceptibility maps. Six different combinations of factor maps were evaluated, with varying geomorphological input. Success rates were used to classify the weight maps into three qualitative landslide susceptibility classes. The resulting six maps were compared with a direct susceptibility map, which was made by direct assignment of susceptibility classes in the field. The analysis indicated that the use of detailed geomorphological information in the bivariate statistical analysis raised the overall accuracy of the final susceptibility map considerably. However, even with the use of a detailed geomorphological factor map, the difference with the separately prepared direct susceptibility map is still significant, due to the generalisations that are inherent to the bivariate statistical analysis technique.

Key words: landslide susceptibility, indirect mapping methods, weights of evidence modelling, GIS, geomorphology.

1. Introduction

Slope instability hazard zonation is defined as the mapping of areas with an equal probability of occurrence of landslides within a specified period of time (Varnes, 1984). Normally, a slope instability hazard zonation consists of two different aspects:

- The assessment of the susceptibility of the terrain for landslides, expressing the likelihood that a landslide might occur under the given terrain conditions or parameters.
- The determination of the probability that a triggering event occurs, such as a major rainfall event or an earthquake. A relation is made between the mag-

nitude and return period of the triggering event and the occurrence of landslides, either through historical studies or through physical models.

Many different types of landslide hazard zonation techniques have been developed over the last decades (Hansen, 1984; Varnes, 1984; Soeters and Van Westen, 1996; Leroi, 1996; Aleotti and Chowdury, 1999). Most of the published literature on landslide hazard mapping actually only deals with landslide susceptibility mapping, or at best spatial probability assessment. It is mostly very difficult to include the temporal probability in the analysis of larger areas, due to the heterogeneity of the subsurface conditions, which are required for physical modelling, or the absence of a complete historic record of both landslide occurrences as well as rainfall and earthquake records (Mulder, 1991; Terlien, 1996).

Generally speaking landslide hazard zonation techniques can be subdivided into direct and indirect methods. In direct mapping the geomorphologist, based on his experience and knowledge of the terrain conditions determines the degree of susceptibility directly. Indirect mapping uses either statistical models or deterministic models to predict landslide prone areas, based on information obtained from the interrelation between landslide conditioning factors and the landslide distribution. The increasing popularity of Geographic Information Systems over the last decades has lead to a majority of studies, mainly using indirect susceptibility mapping approaches (Aleotti and Chowdury, 1999). GIS is very suitable for indirect landslide susceptibility mapping, in which all possible landslide contributing terrain factors are combined with a landslide inventory map, using data-integration techniques (Van Westen, 1993; Bonham-Carter, 1994; Chung *et al.*, 1995). One of the simplest methods, the landslide information value method (Yin and Yan, 1988) is defined as the logarithm of the ratio between the density of landslides in a class over the density of landslides for the whole study area. Chung and Fabbri (1993, 1999) developed statistical procedures under the name of predictive modelling, applying favourability functions on individual parameters. Using these statistical methods, terrain units or grid cells are transformed to new values representing the degree of probability, certainty, belief or plausibility that the respective terrain units or grid cells may contain or can be expected to be subject to a particular landslide in the future.

The use of indirect methods such as bivariate statistics has a number of drawbacks. One of these is the tendency to simplify the factors that condition landslides, by taking only those that can be relatively easily mapped in an area, such as slope angle or lithology. Another problem is related to generalisation, assuming that landslides happen under the same combination of factors throughout the study area. The third problem is related to the fact that each landslide type will have its own set of causal factors, and should be analysed individually (Kojima *et al.*, 2000). A fourth problem is the lack of expert opinion on different landslide types and processes, which is common if these methods are applied by GIS-experts, and not by earth scientists. For most earth scientists it is also very difficult to formulate

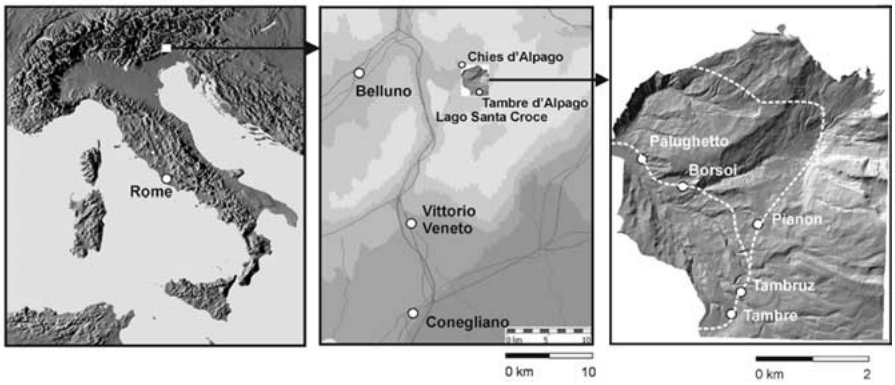

Figure 1. Location of the study area.

their expert knowledge that they applied in the direct susceptibility mapping, into clear decision rules.

This study intends to contribute to bridging the gap between the direct and indirect landslide susceptibility zonation methods, by evaluating the importance of geomorphological information in the generation of landslide susceptibility maps, using GIS supported indirect bivariate statistical analysis.

2. The Study Area

The study was carried out on a test site in the Alpago basin, located to the East of Belluno, Italy (Figure 1). The study area, with a size of 20.8 km^2, consists of two watersheds: the Borsoia watershed to the South and the Boccolana watershed in the North. A steep mountain ridge, consisting of limestone that rises up to more than 2,000 meters a.s.l, forms the northeastern boundary of the area. The western part is underlain by flysch, and has a more gentle, undulating morphology with an average altitude around 1,200 meters. A detailed geological description of the area is given by Mantovani *et al.* (1976).

The geomorphology of the area is dominated by glacial and denudational landforms. Many different glacial and fluvioglacial depositional and erosional landforms give evidence of a complex deglaciation history, where the regional Piave glacier interacted with the local Borsoia glacier. An overview of the various deglaciation phases is given by Van Westen *et al.* (2000b).

Many landslides are found, varying in type, activity and age. On the basis of geomorphological indicators, such as glacial reworking, a number of the landslides located at higher altitudes were interpreted as pre-glacial (Van Westen *et al.*, 2000b), where others are interpreted as being from late glacial, early Holocene or late Holocene times.

The glacial landforms and materials have played an important role in the formation of landslide in the area, as well as the underlying flysch rocks. Some of the

landslides in the area show geomorphological evidence that they have been formed during, or shortly after the last glaciation, for example by glacial or fluvoglacial reworking of the toe of the landslide (Van Westen *et al.*, 2000a). A number of large translational landslides are found which are controlled by the dip of the strata in the flysch formation. For more information on the geomorphology of the study area, the reader is referred to the colour map attached to this volume.

3. Geomorphological Mapping

As part of the study a detailed geomorphological map was prepared, based on a detailed photo-interpretation and extensive fieldwork. A geomorphological interpretation was made using several sets of airphotos, ranging from 1954 to 1980, having a scale of 1:10,000 to 1:30,000.

For the selection if the optimal method to be used for detailed GIS-based geomorphological mapping in mountainous terrain, a review was made of existing mapping methods and classification systems. Overviews of conventional geomorphological mapping systems at medium and large scales are presented by Demek and Embleton (1978) and Van Zuidam (1986). Unfortunately, there is no universally accepted geomorphological classification system. Comparisons of different systems have been presented by Gilewska (1976), Klimazewski (1982), and Salomé and Van Dorsser (1982,1985). In contrast to the systems applied on regional scales, which almost all involve outlining homogeneous units, the conventional geomorphological mapping systems for scales of 1:25,000 and larger are based on individual representation of features such as morphometry, morphography, drainage, genesis, chronology, materials, or processes with different symbols, lines, colours, and hatchings. Conventional large scale mapping systems for mountainous areas have been developed for example by Brunsden *et al.* (1975), Kienholz (1977), De Graaff *et al.* (1987) and Canuti *et al.* (1986). Unfortunately, these geomorphological mapping systems cannot be used easily within a GIS, because it requires a redrawing of the symbol-based maps into polygons maps before digitising, and the design of a new classification system for these polygons.

Therefore it was decided to develop a polygon-based classification system for the geomorphological mapping specifically for the Alpago area, and use this in both the photo-interpretation and fieldwork phases. During the development of the classification system, the legend structure for one single geomorphological layer was too complicated, given the detailed scale of mapping (1:5,000). Therefore it was decided to make two individual GIS layers (geomorphological main units and subunits), each one with a more simplified legend. The total geomorphological description of a certain unit is obtained when consulting both layers at the same time in a GIS.

The layer with the geomorphological main units consisted of 425 different polygons in 52 legend classes, which show information on the genesis and material types, and the chronological information (Table III). The layer with the geomor-

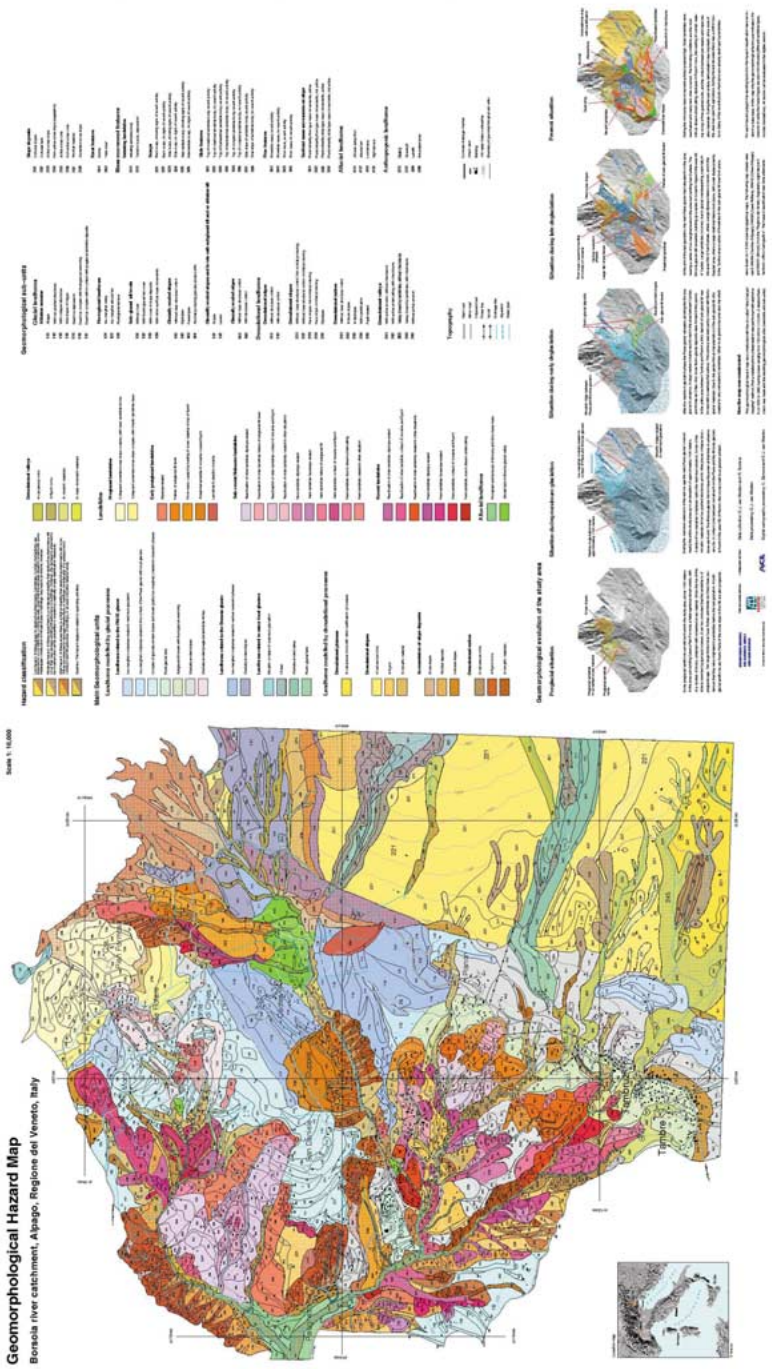

Map 1. Geomorphological hazard map. Borsoia river catchment, Alpago, Regione del Veneto, Italy. Scale: 1:10,000.

phological subunits consisted of 1774 different polygons in 81 legend classes, which contain detailed descriptions on each slope segment. Geomorphological subunits are the smallest sections of the terrain that can be presented on a large-scale map. A geomorphological subunit consists of one landform, for which the genesis, together with morphographical characteristics is given. Both geomorphological layers contain information on the landslides in the study area. In the geomorphological main unit layer, information is given on the relative age of the movement, and the main causal factors, whereas a detailed description of the landslide components and activity is given in the geomorphological subunits.

The geomorphological layer method is a specifically designed for the use with a GIS, where the full overview of the geomorphology can be obtained by simultaneously reading the information from several data layers. A paper version of the geomorphological hazard map was made with the help of a digital cartographic package. The resulting colour map at scale 1:10,000 is attached in this volume of the Journal.

4. Direct Landslide Susceptibility Mapping

On the basis of the geomorphological maps a landslide susceptibility map was made using a direct mapping approach (Soeters and Van Westen, 1996). During the fieldwork the susceptibility degree of each individual polygon of the geomorphological map was evaluated on the basis of geomorphological criteria, such as the presence of evidences of mass movement activity (e.g. scarps, cracks, tilted trees, moved blocks etc.), the freshness and relative age of these features, the location near other polygons that might have influence (e.g. location below a scarp, or above a retrogressive landslide), or the presence of other factors that might cause slope instability (such as slope deposits, subglacial tills, steep slopes, water stagnation etc.).

The actual landslide susceptibility map was made after the digitising of the geomorphological layers. While consulting the information of both layers, a new layer was generated, by reassigning classes to the geomorphological subunits. Whenever two adjacent polygons had the same susceptibility degree, their boundary line was deleted. The resulting susceptibility map consisted of 195 polygons with unique identifiers. For each polygon the deciding factors for the susceptibility classification were recorded in an attribute table. This table also contained information on the process type expected (small rockfall, large rockfall, landslides, flowslides, and flows), as well as on the degree of susceptibility. The susceptibility legend was kept simple, using only three levels (high, moderate, and low), which were based on the following definitions:

- In the areas with a low susceptibility no destructive phenomena are expected to occur within the coming years, given that the land use situation remains the same. Inadequate construction of infrastructure or buildings may lead to problems, however.

- In the polygons with a moderate susceptibility there is a moderate chance that destructive phenomena will occur within the coming years that may damage infrastructure or buildings. However, the damage is expected to be localized and can be prevented or evaded by relatively simple stabilization measures.
- The areas having a high susceptibility have a high chance that destructive phenomena will occur within the coming years. These are expected to damage infrastructure or buildings considerably. It is advised not to construct new infrastructure or buildings, or at least only after detailed study.

The GIS allows for the consultation of the landslide susceptibility layer in combination with other types of information, such as the geomorphological layers and as well as lithology, slope angle and land use.

5. Indirect Landslide Susceptibility Mapping

Indirect landslide susceptibility mapping is characterized by predicting the degree of landslide susceptibility on the basis of the factors that condition the occurrence of landslides factors, such as lithological units, slope classes or land use types. Many different indirect methods have been applied, which can be subdivided into heuristic, statistical and deterministic approaches (Soeters and Van Westen, 1996).

In the statistical approach all landslide conditioning factors that can be mapped, are entered into a GIS and converted from vector to raster maps. After this an overlay is made of each factor map with the landslide inventory map and the frequency statistics are calculated for the combinations of the two maps. The importance of each factor for the occurrence of landslides is judged by comparing the density of landslides within the area occupied by the factor, with the landslide density in the entire area. In this study the weights of evidence method (Bonham-Carter, 1994) was selected for the indirect landslide susceptibility assessment. In this method positive and negative weights (W_i^+ and W_i^-) are assigned to each of the different classes into which a factor map is classified (e.g. each lithological unit within a lithology map), and are defined as:

$$W_i^+ = \log_e \frac{P\{B_i|D\}}{P\{B_i|\bar{S}\}} \tag{1}$$

and

$$W_i^- = \log_e \frac{P\{\overline{B_i}|S\}}{P\{\overline{B_i}|\bar{S}\}} \tag{2}$$

where, B_i = presence of a potential landslide conditioning factor, $\overline{B_i}$ = absence of a potential landslide conditioning factor, S = presence of a landslide, and $\overline{S_i}$ = absence of a landslide.

The method can be performed using individual factor maps, which only contain two classes, representing the presence or absence of the factor. Since this requires

Table I. Four possible combinations of a potential landslide conditioning factor and a landslide inventory map. $Npix$ = number of pixels

		B_i: Potential landslide conditioning factor	
		(Present)	(Absent)
S: Landslides	Present	$Npix_1$	$Npix_2$
	Absent	$Npix_3$	$Npix_4$

the analysis of many individual maps (e.g. each lithological unit separately) it is more convenient to work with multi-class maps, containing many factors (e.g. all lithological units together in one map).

For each factor, W_i^+ is used for those pixels of a factor (represented as a class in a multi-class map) to indicate the importance of the presence of the factor for the occurrence of landslides. If W_i^+ is positive the presence of the factor is favourable for the occurrence of landslides, and if W_i^+ is negative it is not favourable. W_i^- is used to evaluate the importance of the absence of the factor for the occurrence of landslides. When W_i^- is positive the absence of the factor is favourable for the occurrence of landslides. Weights with extreme values indicate that the factor is a useful one for the susceptibility mapping, while factors with a weight around zero have no relation with the occurrence of landslides. For each factor there are four possible combinations, of which the frequency, expressed as number of pixels, can be calculated with a GIS (Table I).

Based on Equations (1) and (2) the weights of evidence can be written in numbers of pixels as follows:

$$W_I^+ = \log_e \frac{\frac{Npix_1}{Npix_1+Npix_2}}{\frac{Npix_3}{Npix_3+Npix_4}} \tag{3}$$

and

$$W_I^- = \log_e \frac{\frac{Npix_2}{Npix_1+Npix_2}}{\frac{Npix_4}{Npix_3+Npix_4}} \tag{4}$$

The weights of evidence method can be performed rather easily with most GIS software packages. Since the same calculation steps have to be carried out using a number of different maps, the calculation procedure was written in the form of a script file, consisting of a series of GIS commands. The script makes use of variables for carrying out the same set of operations for all maps.

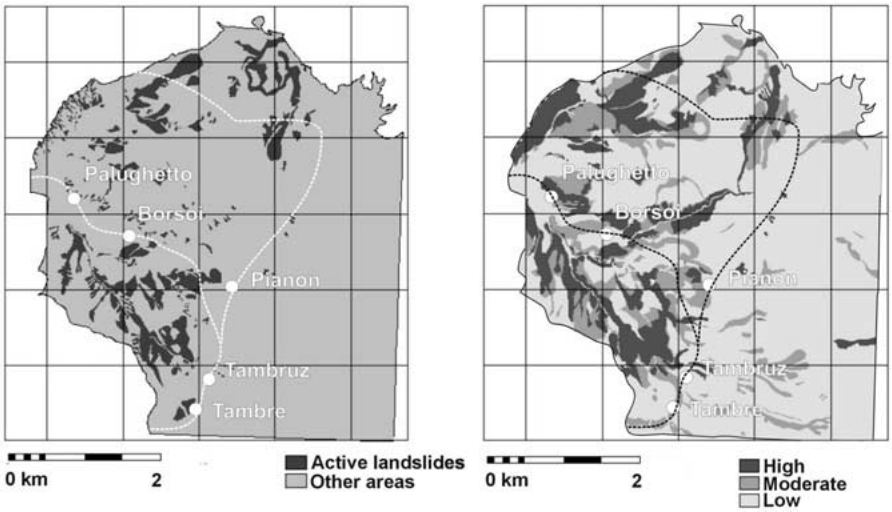

Figure 2. Left: Simplified landslide inventory map used for the indirect hazard assessment, showing only the location of active landslides. Right: Simplified direct susceptibility map.

6. Analysis of the Factor Maps

In order to carry out the weights of evidence modelling in the study area, a landslide inventory map was generated, and a number of maps with information on landslide conditioning factors. As the study is only dealing with landslide susceptibility and not landslide hazard, information on triggering factors, such as rainfall and seismic acceleration were not taken into account. Information on the occurrence of mass movement processes was obtained directly from the geomorphological layers in the GIS. From these layers a separate landslide inventory map was made consisting of 409 polygons with unique identifiers. The map is linked to an attribute table, which contains information on the mass movement type, the dimensions of the mass movement phenomena, and the main causes for the occurrence. For this study the landslide inventory map was simplified to a map displaying only the active landslides in the area (Figure 2). This map was used in the indirect susceptibility assessment as the evidence map. Also the geomorphological susceptibility map was modified so that it only indicated the information related to mass movements of slide and flow type. Other processes, such as rockfall were not left out, since they occur under a different set of conditions and would have to be analysed separately.

For the weights of evidence modelling the following landslide conditioning factor maps were generated (Tables II and III):

- Bedrock map, indicating the main geological units in the areas. This map was digitised from the existing geological map of the study area (Mantovani *et al.*, 1976), after redrawing the units to the 1:5,000 scale topomaps.

- Structural geological map, showing the location of dip-slopes and face-slopes. This map was prepared based on existing geological information and additional fieldwork.
- Surficial materials, showing the types of quaternary deposits. This information was derived through fieldwork and generated from the geomorphological layers in the GIS.
- Land use, prepared by fieldwork, photo-interpretation and the existing information on the 1:5,000 scale topographic maps. Land use is considered to be a landslide conditioning factor, and not a triggering factor, since the land use type might affect the hydrological condition and soil strength.
- Slope angles, in classes of 10 degrees. This map was generated from a Digital Elevation Model. The DEM was made through the interpolation of contour lines from 4 digitised 1:5,000 toposheets, with contour interval of 2.5 meters.
- Distance from roads. This map was made by applying a buffer to the road network, and was classified into two classes (<25 meter from the road, and 25–50 meters from the road). This factor map was generated to test the hypothesis that landslides may be more frequent along roads, due to inappropriate cut-slopes and drainage from the road.
- Distance from streams. Also this map was generated using a buffer, in this case around the stream network, and the same two distance classes were used as for the roads. The hypothesis that was checked was the possible higher landslide frequency along streams, due to undercutting.
- Main geomorphological units, and geomorphological subunits, which were mentioned earlier.

All maps were stored in raster format (1909 rows, 1772 columns) with a pixelsize of 3 meters. The factor maps were all combined with the landslide inventory map (Figure 2) for the calculation of the positive and negative weights.

Since all of the maps are multi-class maps, containing several factors (classes), the presence of one factor (e.g. one specific lithological unit) implies the absence of the other factors of the same map (e.g. lithological map). Therefore in order to obtain the total weight of each factor, the positive weight of the factor itself was added to the negative weight of the other factors in the same map.

The resulting total weights, as shown in Tables II and III, directly indicate the importance of each factor. If the total weight is positive, the factor is favourable for the occurrence of landslides, and if it is negative it is not. As can be concluded from Tables II and III, some of the factors show hardly any relation with the occurrence of landslides, as evidenced by weights close to 0. For example, contrary to what one would expect, most of the slope classes show values that oscillate around zero, without any extreme positive or negative values. This indicates that slope is not a very good predicting factor in this study area. The distance from roads and the distance from streams were both also not very important, as the weights were not very pronounced. With respect to the bedrock types, the analysis proved that the presence of calcareous rocks is a clear indicator for the absence of landslides, as

this factor had the highest negative total weight (−8.5), followed by the presence of rockfall (−7.9) and scree (−4.9). This is also due to the fact that all active rockfall processes were removed from the training data set, and were not included in the analysis.

The geomorphological units (Table III) had much more pronounced weights than the other factor maps (Table II), as can be seen from the very high negative and high positive weights. The geomorphological units dealing with the various landslide phases (pre-glacial, early postglacial, sub-recent Holocene and recent) obviously have a high relation with the occurrence of active landslides, either as new ones or as reactivations of old landslide complexes. The geomorphological subunits showed an even higher relation with maximum weights up to +14. The results are not shown here, due to the extensive legend of the geomorphological subunit map. However, the geomorphological sub-units were mapped in such a detailed way that the high positive weights nearly completely coincide with the landslide pattern, and therefore were not considered useful indicators the prediction of new landslides.

7. Selection of Scenarios

Based on the weights presented in the previous section, a number of combinations of factor maps were selected, in order to test their "predictive power". For each combination the weights of the individual maps were added. The following combinations were selected for further analysis:

- Map 1. Only the factors related to bedrock types and slope classes were used, since in many landslide susceptibility studies these are considered to be the most important landslide conditioning factors (e.g. Brabb, 1984).
- Map 2. The following factor maps were used: structural geology, bedrock type, slope classes, land use and distance from drainage. These factors were used to test how good the prediction would be if geomorphological input data is not used.
- Map 3. For this map the same factor maps were used as in the previous case, with addition of the surface material map. The reason for this is that surface material in this area is considered to be an important landslide-conditioning factor, which also has a clear relation with the geomorphology.
- Map 4. This map was made using the same combination of map 3, but with the addition of the main geomorphological units.
- Map 5. Here, instead of the main geomorphological units, the geomorphological sub-units were used as factor map, combined with the same factors as for map 3.
- Map 6: Weights are only used from the geomorphological maps (main units and subunits), without any other additional factor map.

The "predictive power" of the resulting 6 combination maps was tested by analysing their success rate (Chung and Fabbri, 1999). The success rate is calculated

Table II. Weights for non-geomorphological factors, as calculated by the weights of evidence modelling

Factor Map	Factor (Class)	Total Weight
Structural geology	Dip-slope	1.514627
	Face-slope	0.406060
Surficial materials	Ablation moraine	−2.997582
	Subglacial till	0.798947
	Fluvio-glacial material	−5.229821
	Alluvial materials	−4.365125
	Colluvial material	−5.234163
	Scree	−4.932881
	Cemented scree	1.092740
	Rockfall material	−7.857759
	Landslide material (undifferentiated)	1.563517
	Landslide material from flysch	1.231779
	Landslide material from moraine	1.424658
	Landslide material from moraine and flysch	1.987710
	Landslide material from scree and flysch	−1.546675
	Landslide material from subglacial till	4.367070
	Landslide material from weathered flysch	1.868644
Bedrock	Calcareous rocks	−8.518484
	Flysch	1.272424
Land use	Bare	1.322403
	Bare with sparse shrubs	0.931164
	Grassland	−0.961017
	Grass land (swampy)	2.076442
	Shrubs	0.829082
	Forest	0.029859
	Forest (reforested)	−1.325931
	Grassland and agriculture	−1.882213
	Settlement	−0.103685
Slope	0–10 degrees	−0.413311
	10–20 degrees	0.093273
	20–30 degrees	0.048432
	30–40 degrees	−0.029504
	40–50 degrees	0.254631
	50–60 degrees	0.241418
	60–70 degrees	−0.392213
	70–80 degrees	−2.433674
Distance from roads	<25 m from road	−0.271342
	25–50 m from road	−0.094518
Distance from streams	<25 m from drainage	0.739747
	25–50 m from drainage	0.541094

Table III. Legend of the main geomorphological units, and the weights, as calculated by the weights of evidence modelling

Code	Geomorphological group	Geomorphological unit	Total weight
111	Landforms related to the PIAVE glacier	Ice-marginal complexes related to maximum glaciation	−8.497910
112		Ice-marginal complexes related to the contact of the Piave glacier with local glaciers	−6.763876
113		Complex of glacially eroded slopes and levels (partly ice-marginal) related to recession phases	−2.137759
114		Fluvio-glacial fans	−5.617430
115		Subglacial till levels with fluvio-glacial reworking	−0.211804
116		Glacially eroded slopes	−1.085356
117		Glacially eroded pre-glacial landslide niches	0.633573
121	Landforms related to the Borsoia glacier	Ice-marginal complexes related to various recession phases	−9.586844
122		Glacially eroded slopes	−2.618129
131	Landforms related to minor local glaciers	Morainic complex of maximum glaciation	−5.844747
132		Glacial cirque	−8.092548
133		Glacially eroded valley	−8.987155
134		Fluvio-glacial fans	−6.464728
211	Denudational plateaus	In calcareous rocks with minor karstification processes	−8.495727
221	Denudational slopes	In calcareous rocks	−10.736714
222		In flysch	−1.161314
223		In morainic material	0.385285
231	Accumulation of slope deposits	Scree slopes	−7.304544
232		Rockfall deposits	−7.900251
233		Colluvial slopes	−7.759841
241	Denudational niches	In calcareous rocks	−8.362938
242		In flysch rocks	0.723635
243		In morainic materials	2.007113
251	Denudational valleys	In calcareous rocks	−5.806453
252		In flysch rocks	1.163205
253		In morainic materials	−0.270045
254		In mass movement materials	0.788522
311	Pre-glacial landslides	Collapsed cemented scree slope complex, with clear landslide blocks	1.464854

Table III. Continued

Code	Geomorphological group	Geomorphological unit	Total weight
312		Collapsed cemented scree slope complex, with chaotic landslide mass	−7.147784
321	Early postglacial landslides	Dipslope related	0.133656
322		Failure of subglacial till level	1.487659
323		Flow-mass, caused by loading of scree material on top of flysch	1.380578
324		Rotational landslide in moraine covered flysch	−1.829337
325		Landslide in ablation moraine	−1.562957
330	Sub-recent Holocene landslides	Reactivation of older landslide: dipslope related	0.673034
331		Reactivation of older landslide: failure of subglacial till level	−0.187895
332		Reactivation of older landslide: contact of moraine and flysch	2.918090
333		Reactivation of older landslide: related to other situations	0.640132
334		Dipslope related	3.159034
335		Faceslope related	2.517143
336		Failure of subglacial till	2.423631
337		Contact of moraine and flysch	1.840670
338		Due to stream undercutting	−1.584268
339		Related to other situation	2.199059
341	Recent landslides	Reactivation of older landslide: dipslope related	8.602759
342		Reactivation of older landslide: contact of moraine and flysch	5.131376
344		Dipslope related	9.437425
345		Faceslope related	2.797559
346		Contact of moraine and flysch	8.483261
347		Due to stream undercutting	10.475438
410	Floodplain and terraces	Of Borsoia and Boccolana rivers	−5.178649
420	Alluvial fans	In Borsoia glacial valley	−7.964455

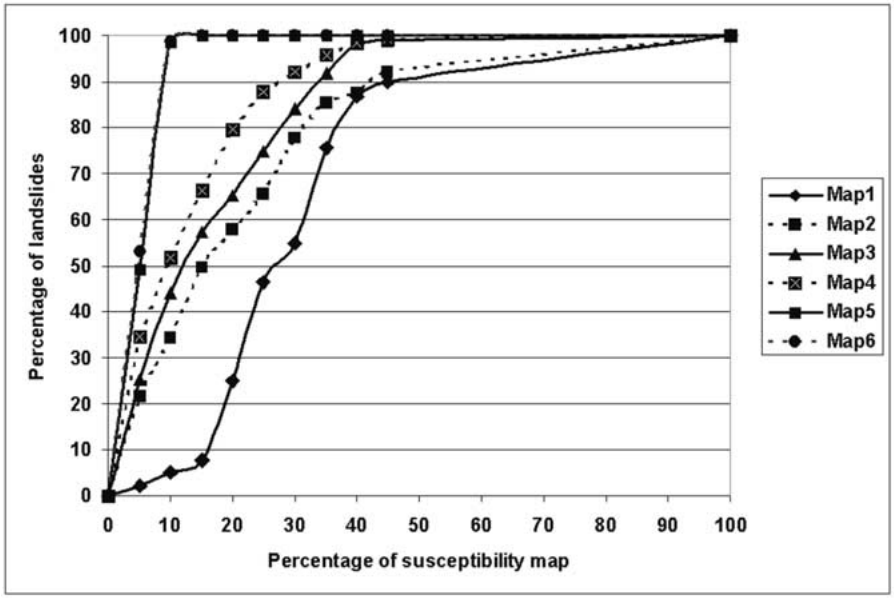

Figure 3. Success rates calculated for the 6 different scenarios. The Y-axis indicates the percentage of all landslides in the study area, and the X-axis indicates the percentage of the susceptibility map ordered in classes with decreasing weights of evidence.

by ordering the pixels of a susceptibility map in a number of classes, from high to low values, based on the frequency information from the histogram. After that an overlay is made with the landslide inventory map, and the joint frequency is calculated. The success rate (Figure 3) indicates how much percentage of all landslides occurs in the classes with the highest values of the different combination maps. In the case of map 4, for example, 50 percent of all landslides are predicted by 10 percent of the classes with the highest value in the susceptibility map, and 90 percent of all landslides occur within the classes covering 30 percent of the map.

As can be seen from Figure 3, the success rate improves from map 1 to map 6. So the more detailed geomorphological information is used, the better is the spatial prediction capacity. Since no multi- temporal landslide data set was available, it was not possible to calculate the prediction rate (Chung and Fabbri, 1999). The procedure for the generation of a prediction rate is similar to that of the success rate, with the main difference that a more recent landslide inventory map is used to check if the landslides indeed have occurred in the areas indicated as highly susceptible. However, the success rate by itself is also a useful indicator for the quality of the map, although it merely shows how good the resulting weight scores can explain the input landslide pattern that was used to calculate them.

It is clear from Figure 3 that in the Alpago area the combination of only slope and geology will not lead to an acceptable result. It is also interesting to observe that the use of geomorphological information improves the success rate consid-

erably. The use of the geomorphological main-units is preferred over the more detailed sub-units, because the latter ones will nearly lead to a resulting map that is almost similar as the input landslide pattern, and therefore has no large prediction power in areas that are not covered by landslides yet.

The success rate curves were also used to classify each of the 6 weight maps into three classes (high, moderate and low susceptibility), by taking a fixed percentage of landslides, and using the corresponding weight value as threshold. For the high susceptibility class the threshold was set at 75 percent of all landslides. For the moderate susceptibility class this was done at 15 percent of the landslides (90% of the total), and for the low susceptibility class at the remaining 10 percent. The six classified maps are shown in Figure 4.

The spatial pattern of the 6 maps is quite different, although all of them have classified the limestone area in the east as low susceptibility. From Map 1 to Map 6, with increasing importance of geomorphological information, the size of the high and moderate susceptibility areas is decreasing. The susceptibility map made only by combining slope classes and lithology (Figure 4A) gives a very poor result, with a randomly distributed high susceptibility class. The maps, which are based on the very detailed geomorphological information (Figures 4E and F), show a near complete overlap with the original landslide map, with very small or even absent moderate classes.

8. Comparison of Direct and Indirect Susceptibility Maps

Finally, the accuracy of the six classified susceptibility maps (Figure 4) was evaluated by comparing them with the direct susceptibility map (Figure 2). This was done by calculating a confusion matrix for each of the six maps, followed by a calculation of the accuracy. It was assumed that the direct susceptibility map represent the "true" situation, since it was carefully prepared by experts, based on many field observations (Van Westen *et al.*, 2000a). The results are shown in Table IV.

The overall accuracy of the six indirect susceptibility maps was calculated by dividing the area (expressed as number of pixels) that was classified identically as the in the direct map (the diagonals in Table IV) over the total area (total number of pixels) in the study area. The following overall accuracy values were obtained for map 1 to map 6: 52%, 63%, 73%, 72%, 76% and 76%.

9. Discussion and Conclusions

The analysis indicated that the use of detailed geomorphological factor maps raised the overall accuracy of the susceptibility maps from 52 to 76 percent. The accuracy of the high susceptibility classes demonstrates this even more. The range is there from 27 percent for map 1 to 76 percent for map 5 and 6. It is clear from these results that in the Alpago area the combination of only slope and geology will not lead

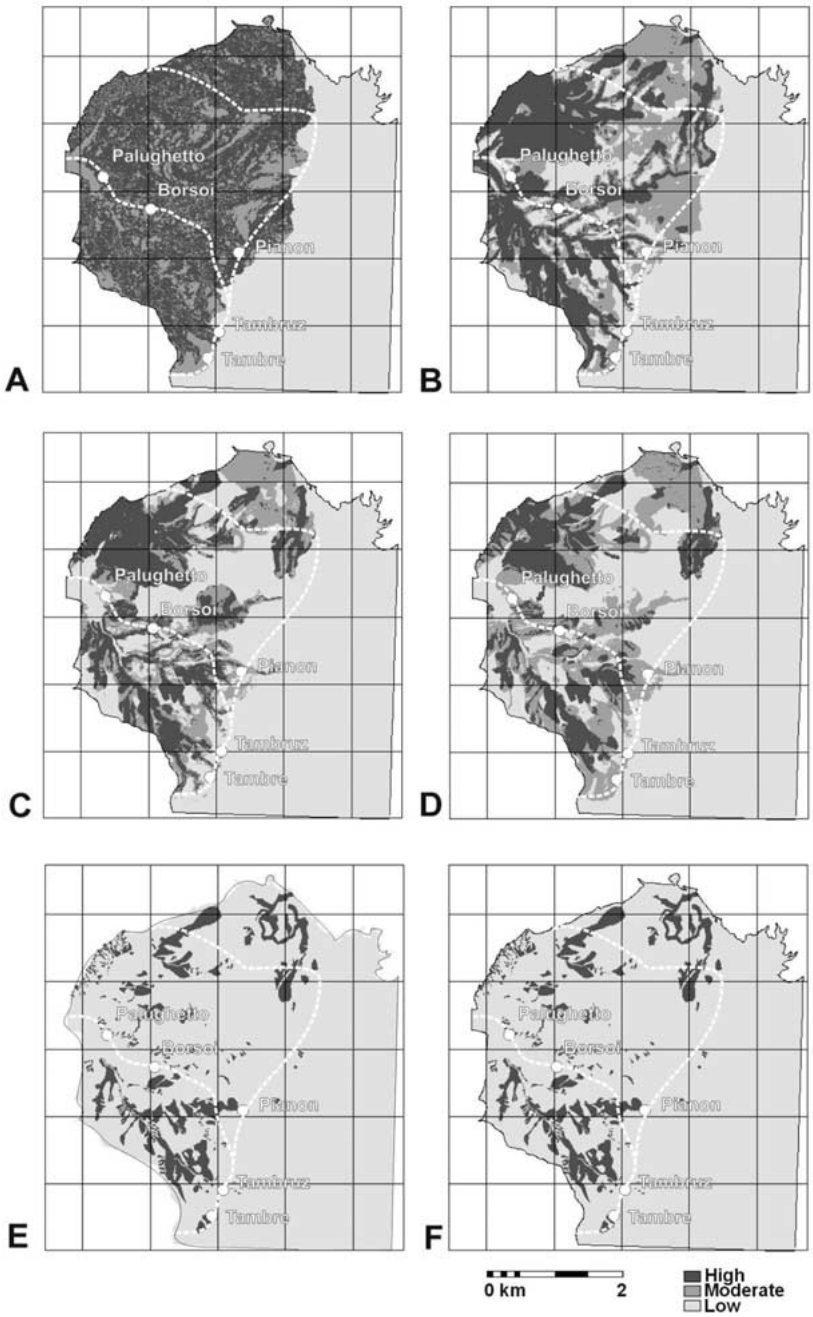

Figure 4. The classified susceptibility maps for the six different map combinations. A = Map 1, B = Map 2, C = Map 3, D = Map 4 , E = Map 5 and F = Map 6. See text for explanation.

Table IV. Confusion matrices for the six indirect susceptibility maps. The number of pixels are given for the combinations of the susceptibility classes of the six indirect maps with those of the direct map

	INDIRECT SUSCEPTIBILITY MAP 1				
DIRECT MAP	Low	Moderate	High	Reliability	
	Low	886689	268517	444431	0.55
	Moderate	81139	55214	218777	0.16
	High	13022	86912	247897	0.71
	Percent of map	42.62	17.83	39.55	
	Accuracy	0.90	0.13	0.27	
	INDIRECT SUSCEPTIBILITY MAP 2				
DIRECT MAP	Low	Moderate	High		
	Low	1087324	172624	339689	0.68
	Moderate	133950	54649	166531	0.15
	High	29139	32428	286264	0.82
	Percent of map	54.32	11.27	34.40	
	Accuracy	0.87	0.21	0.36	
	INDIRECT SUSCEPTIBILITY MAP 3				
DIRECT MAP	Low	Moderate	High		
	Low	1330828	37745	159459	0.84
	Moderate	131363	48180	152188	0.19
	High	33287	25080	264710	0.76
	Percent of map	64.96	4.82	30.22	
	Accuracy	0.89	0.43	0.46	
	INDIRECT SUSCEPTIBILITY MAP 4				
DIRECT MAP	Low	Moderate	High		
	Low	1336484	103694	159459	0.84
	Moderate	135042	67900	152188	0.19
	High	24696	58424	264710	0.76
	Percent of map	65.00	9.99	25.02	
	Accuracy	0.89	0.30	0.46	
	INDIRECT SUSCEPTIBILITY MAP 5				
DIRECT MAP	Low	Moderate	High		
	Low	1577744	0	21765	0.99
	Moderate	321158	0	33956	0.00
	High	173242	0	174529	0.50
	Percent of map	90.00	0	10.00	
	Accuracy	0.76	?	0.76	
	INDIRECT SUSCEPTIBILITY MAP 6				
DIRECT MAP	Low	Moderate	High		
	Low	1578498	0	22082	0.99
	Moderate	321219	0	33895	0.00
	High	172851	0	174921	0.50
	Percent of map	89.99	0	10.01	
	Accuracy	0.76	?	0.76	

to an acceptable result, because the lithology is rather homogeneous and landslides occur on different slope angles. The use of other factor maps, such as structural geology and land use increases the accuracy, but the main step of improvement in this area is made by the inclusion of geomorphological information.

One aspect that was clearly demonstrated in this study was that every study area has its own particular set of factors, which condition landslides. From the results it is also clear that the use of the very detailed geomorphological sub-units will lead to an unacceptable limitation of the high susceptibility areas, nearly overlapping with the input landslide pattern, so the resulting susceptibility maps (Maps 5 and 6) therefore are not considered to be very useful for the prediction of new landslides. This is due to the fact that the geomorphological subunits map is so detailed, that it describes the terrain at a slope facet level, and that all landslides are described within this map as separate legend units (see attached colour map). If the geomorphological subunit map would have been used as the only factor map in the analysis, the success rate would have been very large and the overall accuracy would have been 100%. However, the resulting susceptibility map would have been identical to the landslide inventory map, and therefore would not have any use for predicting new landslides. For this reason the use of the geomorphological main-units is considered to be the best approach in this area.

However, even with the use of geomorphological factor maps, the difference with the direct susceptibility map is still significant. The maximum accuracy reached with the indirect methods does not exceed 76 percent. This is due to a number of factors. One of the most important is the generalisation that is inherent to the bivariate statistical analysis technique, assuming that landslides are conditioned by the same combination of factors throughout the area. The direct geomorphological mapping, on the other hand, is able to evaluate subtle changes in the landslide conditioning factors, and make specific judgements for each particular site. The direct susceptibility map also includes factors that are difficult to include within the bivariate statistical method, such as the areas above or below active scarps, where landslides may extend in the future.

The bivariate statistical method gives a satisfactory combination of the (subjective) professional direct mapping and the (objective) data driven analytical capabilities of a GIS. The main advantage of bivariate statistical procedures is that the professional, who executes the analysis, determines the factors or combinations of factors used in the assessment. This enables the introduction of expert opinion into the process. The methodology asks for a careful confrontation of the susceptibility assessment with the “real world” and an adaptation of decision rules there where differences are observed, this based mostly on experience driven criteria. Bivariate statistics are a useful tool in the assessment of landslide susceptibility, but can best be used as a supporting tool to make quantitative estimations of the importance of the various factors involved. The actual generation of the susceptibility maps is best done by knowledge driven methods, such as multi-class index overlaying or fuzzy logic methods.

References

Aleotti, P. and Chowdury, R.: 1999, Landslide hazard assessment: summary review and new perspectives, *Bull. Eng. Geol. Envir.*, **58**(1), 21–44.

Bonham-Carter, G.F.: 1994, Geographic Information Systems for Geoscientists; modelling with GIS, *Comp. Meth. Geos.*, Vol. 13, Pergamon Press, pp. 398.

Brabb, E.E.: 1984, Innovative approaches to landslide hazard and risk mapping, *Proceedings 4th International Symposium on Landslides*, Toronto, Canada, Vol. 1, pp 307–324.

Brunsden, D., Doornkamp, J. C., Fookes, P. G., Jones, D. K. C., and Kelly, J. M. H.: 1975, Large scale geomorphological mapping and highway engineering design, *Quarterly. Jrnl. Eng. Geol.* **8**, 227–253.

Canuti, P. *et al.*: 1986, Slope stability mapping in Tuscany, Italy, In: V. Gardiner (ed.), *International Geomorphology. Part 1*, Wiley & Sons, New York, pp. 231–239.

Chung, C. F. and Fabbri, A. G.: 1993, The representation of geoscience information for data integration, *Nonrenewable Resources* **2:2**, 122–139.

Chung, C. J., Fabbri, A., and Van Westen, C. J.: 1995, Multivariate regression analysis for landslide hazard zonation, In: A. Carrara and F. Guzetti (eds), *Geographical Information Systems in Assessing Natural Hazards*, Kluwer, pp 107–133.

Chung, C. F. and Fabbri, A. G., 1999, Probabilistic prediction models for landslide hazard mapping, *Photogrammetric Engineering & Remote Sensing* **65**(12), 1389–1399.

De Graaff, L. W. S., de Jong, M. G. G., Rupke, J., and Verhofstad, J.: 1987, A geomorphological mapping system at scale 1:10.000 for mountainous areas, *Zeitschrift für Geomorphologie. N.F.* **31**(2), 229–242

Demek, J. and Embleton, C. (eds): 1978, *Guide to medium-scale geomorphological mapping*, IGU Commission on Geomorphological Survey and Mapping. E. Schweizerbart'sche Verlagsbuchhandlung, Stuttgart, Germany, 348 pp.

Gilewska, S.: 1976, Different methods of showing the relief on detailed geomorphological maps, *Zeitschrift für Geomorphologie* **11**(4), 81–490.

Hansen, A.: 1984, Landslide Hazard Analysis, In: Brunsden, D. and Prior, D. B. (eds), *Slope Instability*, Wiley & Sons, New York, pp. 523–602.

Kienholz, H.: 1977, *Kombinierte Geomorphologische Gefahrenkarte 1:10.000 von Grindelwald. Geographica Bernensia G4*, Geographisches Institut Universität, Bern, Switzerland.

Klimazewski, M.: 1982, Detailed geomorphological maps, *ITC-Journal* 1982–3, pp. 265–272.

Kojima, H., Chung, C. J., and Van Westen, C. J.: 2000, *Strategy on the landslide type analysis based on the expert knowledge and the quantitative prediction model*, ISPRS congress 2000. International Archives of Photogrammetry and Remote Sensing, Vol. XXXIII, Part B7, pp. 701–708.

Leroi, E.: 1996, Landslide hazard – Risk maps at different scales: Objectives, tools and developments, In: Senneset (ed.), *Landslides*, Proceedings, 7th International Symposium on Landslides, Trondheim, Norway, 17–21 June 1996. Balkema, Rotterdam, pp. 35–51.

Mantovani, F. Panizza, M., Semenza E., and Piacente, S.: 1976, L'Alpago (Prealpi Bellunesi). Geologia, Geomorfologia, Nivopluviometria, *Boll. Soc. Geol. It.* **95**, 1589–1656.

Mulder, H. F. H. M.: 1991, *Assessment of landslide hazard*, Nederlandse Geografische Studies, 124, University of Utrecht. 150 pp.

Salomé, A. I. and Van Dorsser, H. J.: 1982, Examples of 1:50.000 scale geomorphological maps of part of the Ardennes, *Zeitschrift für Geomorphologie Bnd.* **26**(4), 481–489.

Salomé, A. I. and Van Dorsser, H. J.: 1985, Some reflections on Geomorphological Mapping Systems, *Zeitschrift für Geomorphologie Bnd.* **29**(3), 375–380.

Soeters, R. and Van Westen C. J.: 1996, Slope Instability Recognition, Analysis and Zonation, In: Turner, A. K. and Schuster, R. L. (eds), *Landslides, investigation and mitigation*, Transporta-

tion Research Board, National Research Council, Special Report 247, National Academy Press, Washington D.C., U.S.A., pp 129–177.

Terlien, M. T. J.: 1996, Modelling spatial and temporal variations in rainfall-triggered landslides, PhD thesis, ITC Publ. Nr. 32, Enschede, The Netherlands, 254 pp.

Varnes, D. J.: 1984, *Landslide Hazard Zonation: a review of principles and practice*, Commission on landslides of the IAEG, UNESCO, Natural Hazards No. 3, 61 pp.

Van Westen, C. J.: 1993, Application of Geographic Information Systems to Landslide Hazard Zonation, Ph-D Dissertation Technical University Delft. ITC-Publication Number 15, ITC, Enschede, The Netherlands, 245 pp.

Van Westen, C. J., Soeters, R., and Sijmons, K.: 2000, Digital Geomorphological landslide hazard mapping of the Alpago area, Italy, *Int. J. Appl. Earth Observ. Geoinformation* **2**(1), 51–59.

Van Westen, C. J., Seijmonsbergen, A. C., and Mantovani, F.: 2000, Comparing landslide hazard maps, *Natural Hazards* **20**, 137- 158.

Van Zuidam, R. A.: 1986, *Terrain classification*, ITC-textbook, ITC, Enschede, The Netherlands.

Yin, K. J. and Yan, T. Z.: 1988, Statistical prediction model for slope instability of metamorphosed rocks, *Proceedings 5th International Symposium on Landslides, Lausanne, Switserland*, Vol. 2, 1269–1272.